NUKLEONIKA 2005;50(1):37–42

ORIGINAL PAPER

Monte Carlo calculations of low energy positrons in silicon

Asuman Aydın

Abstract Theoretical data for positron scattering from a thin silicon film and semi-infinite silicon are presented as a function of incident and outgoing angles and energies. These theoretical data of the scattering processes of low energy positrons penetrating into silicon were performed by Monte Carlo simulation. The simulation is based on the use of different types of differential cross sections for individual elastic and inelastic scattering i) inelastic scattering; Gryzinski's excitation function to simulate the energy loss and Liljequist's model to calculate the inelastic scattering cross section, ii) elastic scattering; the screened Rutherford differential cross section with the spin-relativistic factor. In calculations on positron traversing matter, it is important to know the transmission through medium, their path lengths, and their energy and angular distribution through matter. The simulation results are well agreed with experiments.

Key words Monte Carlo method • positron transmission • backscattering • angular distribution • energy distribution

A. Aydın
Faculty of Science and Literature,
Department of Physics,
Balıkesir University,
10100 Balıkesir, Turkey,
Tel.: +90 266/ 249 33 58-59 ext. 131,
Fax: +90 266/ 245 63 66,
E-mail: aydina@balikesir.edu.tr

Received: 1 March 2004
Accepted: 23 August 2004

Introduction

The penetration of charged particles through matter is determined by the outcomes of countless Coulomb collisions with atoms and atomic electrons. It is a useful schematization to classify these collisions as soft and hard. Soft collisions, with impact parameters large compared to atomic dimensions are extremely numerous, and give rise to small energy losses and deflections. Hard collisions, with small impact parameters are much less frequent and result in large energy losses and deflections. Both types of collisions make essential contributions to the transport process [4]. The dynamics of each individual collision should be known accurately for a reliable Monte Carlo simulation of such events. The atomic collisions of charged particles, as many body problems [13] are very difficult to solve exactly, therefore several approximations, which are valid in various incoming particle energy regions, are made to find solutions.

A low-energy positron beam may be thought as the antimatter complement to the electron beams found in many diagnostic probes and other useful devices. The exciting field of low-energy positron research has been revolutionized by the introduction of slow-positron beams. Once positron is injected into the material, it suffers elastic and inelastic scattering events. Because both scattering processes are important in determining, for example, particle ranges and backscattering probabilities, it is difficult experimentally to study any particular process in isolation. The Monte Carlo simulation technique, in which the particle trajectories are

modeled as random walks, is probably the most basic approach to study the implantation of keV positrons in solids. The accuracy of the Monte Carlo method depends crucially on the modeling of the scattering processes employed in the simulation. A well-developed Monte Carlo model which incorporates the relevant physics can provide a useful approach to modeling the implantation process and calculating the stopping profiles. The success or failure of the model depends on the three physical quantities associated with every collision: the mean free path, the scattering angle and the energy loss.

Numerous scattering models and computer codes to simulate the penetration and energy loss of electrons and positrons through matter by using Monte Carlo methods has been developed for many years. For electrons and positrons energies in the range of keV, the total number of elastic and inelastic collisions suffered by electrons and positrons until being completely stopped is of the order of several hundreds. Such a number of collisions can be simulated by first principles of Monte Carlo procedures in a fast computer.

Attempts have been made to satisfactorily describe the energy and angular distribution of transmitted positrons using Monte Carlo calculations. The most successful so far is the direct simulation technique. In this technique, the statistical nature of elastic and inelastic scattering processes, are taken into account. Elastic and inelastic scattering can be described in different ways. The most basic approach to the penetration of keV positrons in solids is probably the Monte Carlo method in which individual positron trajectories, resulting from a series of random scattering events, are simulated in computer. The Monte Carlo technique has, in fact, described various phenomena (e.g. electron-positron backscattering energy and angular dissipations, in bulk targets or implantation profile, mean penetration depth in semi-infinite targets) with considerable success.

Thus, the direct Monte Carlo simulation approach is very useful for describing scattering processes of keV positrons in solids provided that exact theoretical expressions for individual elastic and inelastic scatterings are given. Although the application of this approach to metal for the penetration of keV positrons has been done with considerable success, the extension of the approach to surface analysis in the lower primary energy region has to be done because the Rutherford type scattering formula [17] is no more valid for the energy region below several keV. The differential cross sections for elastic scattering mostly used the partial wave expansion method [6] instead of the screened Rutherford scattering formula.

For the basic positron scattering interactions more detailed and precise experimental information, in particular the energy and angular distribution of backscattered positrons, is required to establish the validity of existing theories. The aim of the present work is to describe the energy and angular distribution of transmitted and backscattered positrons using Monte Carlo calculations for a thin silicon film and semi-infinite silicon. There is a reasonable amount of experimental data available for electron, representing a large range of incident projectile angles and energies, target species and experimental geometries, but there is not enough experimental data available for positron. Monte Carlo computer simulations are compared with the experimental data for transmission probabilities and these results show good agreement.

Simulation procedure

The screened Rutherford cross section with the spin-relativistic factor [17] and some extra total cross section information at low energies for elastic scattering and Liljequist's model [9] to calculate the total inelastic scattering cross section for inelastic scattering have been used. The energy loss in the inelastic scattering process has been sampled using Gryzinski's excitation function [7]. The detailed description of cross sections has been reported [1, 15]. As is usual in detailed Monte Carlo calculations, a positron is represented by its energy, position coordinate and direction cosines relative to some frame of reference. The energy dependent mean free path between two collisions is given by

$$\frac{1}{\lambda_{tot}} = \frac{N_0 \rho}{A} \Sigma_{tot} \tag{1}$$

where Σ_{tot} is the total cross section

$$\Sigma_{tot} = \Sigma_{el} + \Sigma_{in}. \tag{2}$$

The path length distribution is presumed to collide after travelling a distance from the

$$s = -\lambda_{tot} \ln(q_1) \tag{3}$$

position of the previous scattering event, q_1, being an homogenous random number ($0 < q < 1$). We decide whether the scattering is elastic or not from another random number q_2, if the inequality

$$q_2 \Sigma_{tot} \leq \Sigma_{el} \tag{4}$$

holds, the next collision is elastic. Otherwise, the collision is inelastic. The polar and azimuthal deflection angles for the elastic scattering are decided by using random number q_3 and q_4, as

$$\cos\theta = 1 - 2\eta q_3/(1 + \eta - q_3) \tag{5}$$

where η is the screening angle [1, 14] and

$$\varphi = 2\pi q_4 \tag{6}$$

from which new direction cosines are calculated in the usual way.

The mean energy loss per inelastic scattering event follows from Gryzinski's excitation function [7]. The polar scattering angle is given from the classical binary collision model as

$$\sin^2 \theta = \frac{\Delta E}{E} \tag{7}$$

and the azimuthal one is randomly sampled by using in Eq. (6). New direction cosines after inelastic events are calculated as in the elastic case.

The computer code has been written for infinitely wide slab and semi-infinite geometries and for monoenergetic positron beams. Individual tracks are

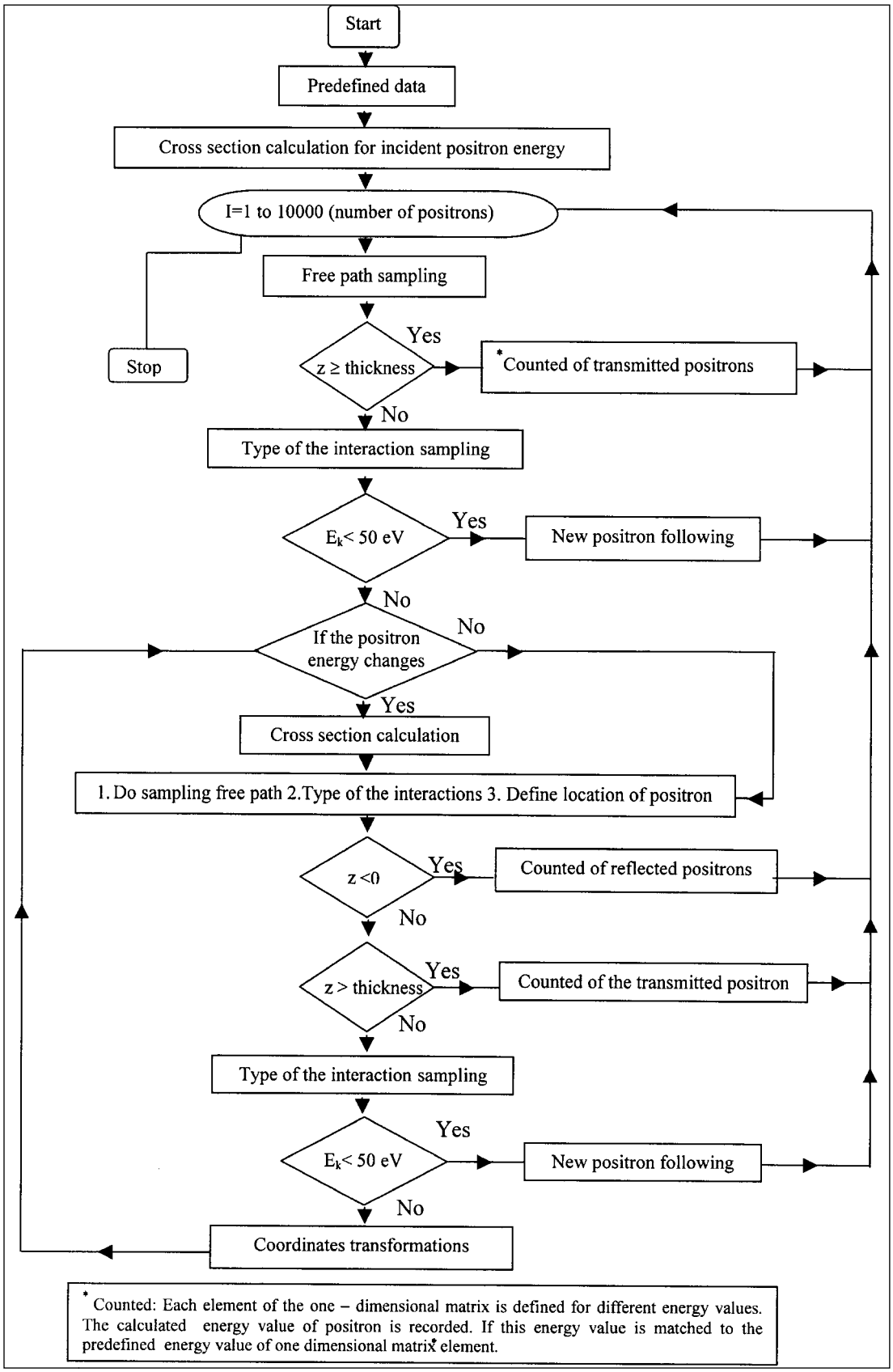

Fig. 1. Flow diagram of the program for reflected and transmitted fractions of positrons and energy distributions.

simulated from until becoming lower than a fixed value. All positrons have backscattered or slowed down below 50 eV. A typical run involves the computation of 10,000 trajectories. The time required to compute a single trajectory clearly depends on the initial energy and on the material. All the calculations have been performed using Intel P4 (2.53 GHz) PC and Turbo Basic compiler. To avoid the sequential correlations, I have used a uniform random number generator of the Turbo Basic compiler, together with the Bays-Durham algorithm Press *et al*. [16].

Results and conclusions

Slab geometry

The measurements of transmission of 1–6 keV energy positrons through films of up to 3000 Å thick Al, Cu and Si were done by Mills and Wilson [12]. For the purpose of examining the present Monte Carlo approach, the experiment of Mills and Wilson [12] was attempted. Furthermore, any experimental and/or theoretical treatments of the energy and angular distributions of transmitted and backscattered positrons for silicon have not been found in the literature yet. Therefore, as far as the backscattering coefficient and transmission rate for thin films are concerned, the conventional Monte Carlo approaches have described the experimental results for electrons much more than positrons [11]. In this study, the angular and energy distributions of both the reflected and transmitted fractions as a function of energy have been simulated.

Transmission rate

Monte Carlo calculations for the transmission rate of 1–10 keV positrons in thin silicon films have been performed for a comparison with the experimental results already published [12]. Figure 1 shows the flow diagram of the program for reflected and transmitted fractions of positrons and energy distributions. The calculated transmission probabilities in silicon are well agreed with those of Mills and Wilson [12]. The results of calculation obtained from the analog Monte Carlo code are shown in Fig. 2. In this figure, the calculated

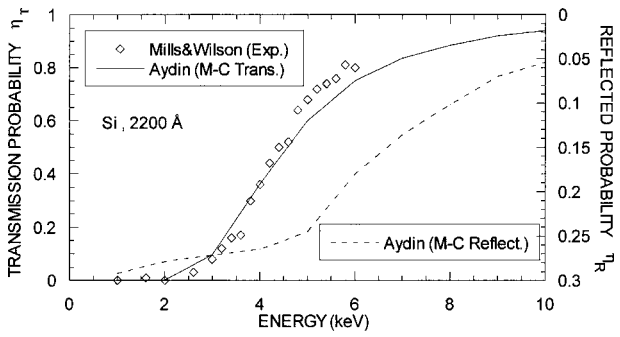

Fig. 2. Relative proportions at 2200 Å thick positrons transmitted η_T (full curve) and reflected η_R (dashed curve) for a thin Si film target. Experimental results (η_T only) are from Mills and Wilson [12].

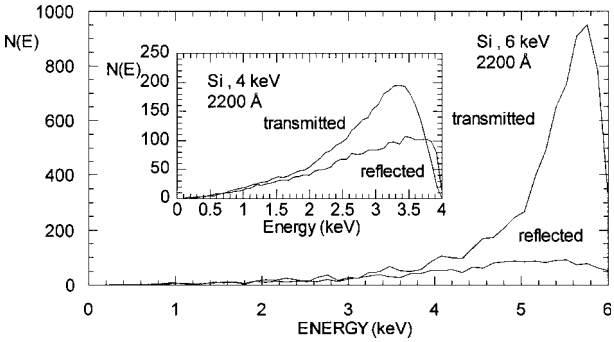

Fig. 3a. Theoretical energy distributions of transmitted and reflected positrons for a thin Si film target 2200 Å thickness at 4 keV and 6 keV energies.

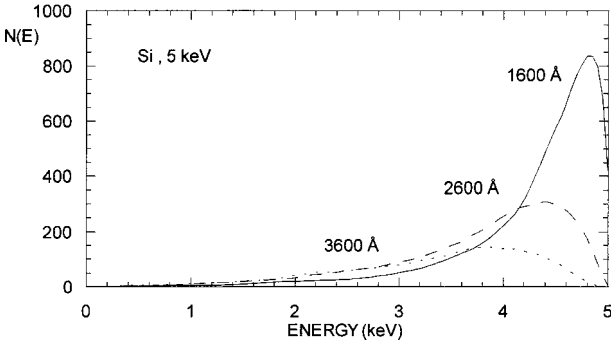

Fig. 3b. Theoretical energy distributions of transmitted positrons for thin Si film targets of various thicknesses at 5 keV energy.

transmission probability was found to be 0.364, while the measurements of Mills and Wilson [12] was 0.360 for 2200 Å thickness at 4 keV energy.

For the accuracy of the presented results, the calculated transmission probability of the positron with kinetic energy 4 keV from a silicon foil of 2200 Å thick, following 10,000 histories 20 times, and found the standard deviation to the mean value as 0.01215. This means that the statistical errors of results are of the order of 1–2 %. The computing time for a typical run is 6–7 min, for example, $E = 4$ keV and 2200 Å thick slab.

Energy and angular distributions

The energy distributions of the transmitted and reflected positrons for various thicknesses of silicon films have been calculated. Figure 3a shows the energy distribution of the transmitted and reflected positrons in thin silicon films at 4 keV and 6 keV energies. In Fig. 3b, it is noticed that half-height widths of the theoretical distributions increase with increasing film thickness.

The angular distribution of transmitted and reflected positrons has also been calculated from the present Monte Carlo calculation for thin silicon films. In practice, the computer program has provided both angular-energy distributions of the transmitted and reflected positrons. However, the restriction on the total number of trajectories, which was, in our case, mainly due to the cost of computing only enabled us to plot the angular or energy distribution separately in order to reduce the statistical deviation in the result. Figure 4a indicates

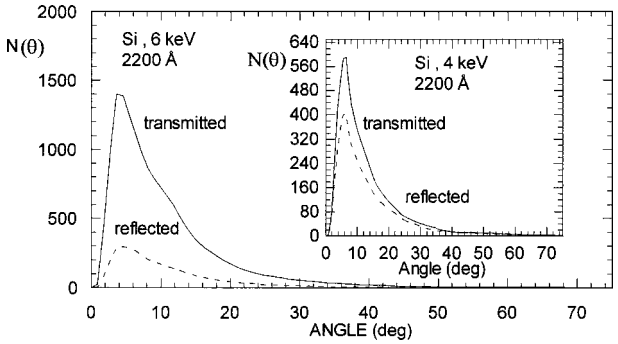

Fig. 4a. Theoretical angular distributions of transmitted and reflected positrons in a thin Si film target 2200 Å thickness at 4 keV and 6 keV energies.

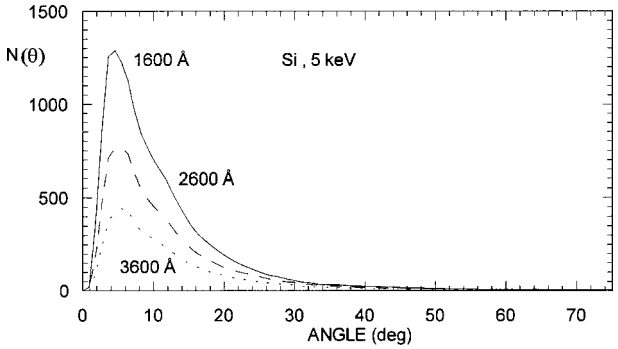

Fig. 4b. Theoretical angular distributions of transmitted positrons for a thin Si film targets of various thicknesses at 5 keV energy.

the angular distribution of transmitted and reflected positrons for 2200 Å thick silicon film at 6 keV. Inset of Fig. 4a shows the angular distributions of transmitted and reflected positrons at 4 keV energy. There is an accumulation at the angles of 0 degree to 10 degree for both 4 keV and 6 keV energies. In addition, at 5 keV, the theoretical angular distributions of transmitted positrons for various thicknesses of thin silicon film targets are indicated in Fig. 4b.

Semi-infinite geometry

Energy and angular distributions

The energy and angular distribution of positrons entering into the semi-infinite silicon target at various angles were also studied. Figure 5a shows the energy distributions of backscattered positron in semi-infinite silicon 0° and 75° incident angles for 10 keV the positron energy. By keeping the angles and energy constant, computed angular distributions of backscattered positron are shown in Fig. 5b. Figure 5c indicates the positron angular distributions for separate incident angles 0°, 30°, 60° at 1 keV and 5 keV. As can be seen in Fig. 5, the energy and angular distributions of backscattered positron increase with increasing incident angle. In another work [2], the backscattering probabilities were calculated using the same geometry used in this study. The backscattering probabilities were, in general, in good agreement with experiment and Monte

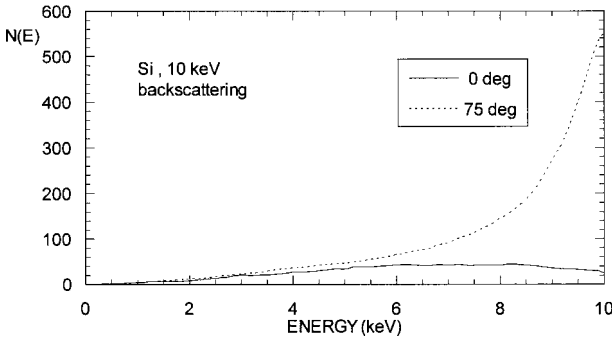

Fig. 5a. Energy distributions of backscattered positrons at 10 keV positron energy and the incident angles of 0°, 75°.

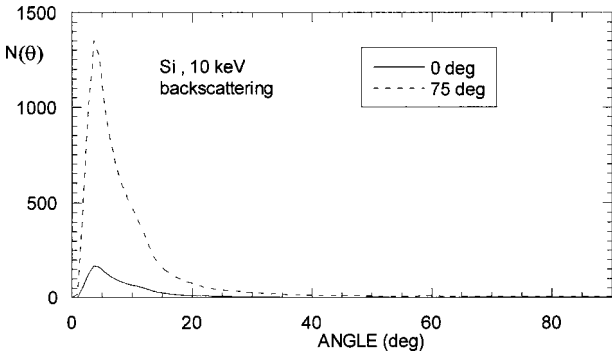

Fig. 5b. Angular distributions of backscattered positrons at the same energy and angles.

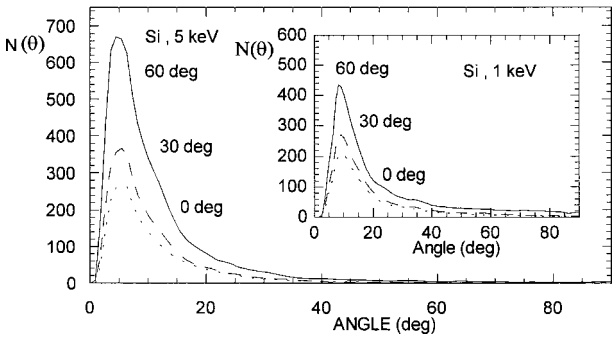

Fig. 5c. Angular distributions of backscattered positrons for 1 and 5 keV positron energies at incident angles of 0°, 30° and 60°.

Carlo results given by Mäkinen *et al.* [10]. Therefore, the details of this calculation can be found in a paper by Aydın [2].

Many papers about the experimental and theoretical results of aluminum can be found in the literature: Baker *et al.* [3], Bouarissa *et al.* [5], Kotera *et al.* [8], Massoumi *et al.* [11], Özmutlu and Aydın [15], Shimuzu and Ichimura [18]. In general implantation profiles in silicon are much like those of aluminum. In Fig. 6a, it can be seen the similarity of particle behavior in aluminum and silicon. This is expected, because silicon is just after aluminum in the periodic table, and silicon has only little larger electron binding energies and four valance electrons as opposed to aluminum. Typical implantation profiles for positrons at various angles and energy are shown in Fig. 6b. Also as can be seen from Fig. 7, the backscattering energy distributions are quite

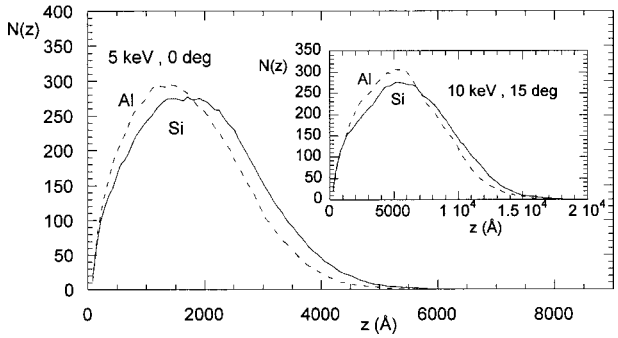

Fig. 6a. Comparison of typical implantation profiles of positrons in the semi-infinite Al and Si.

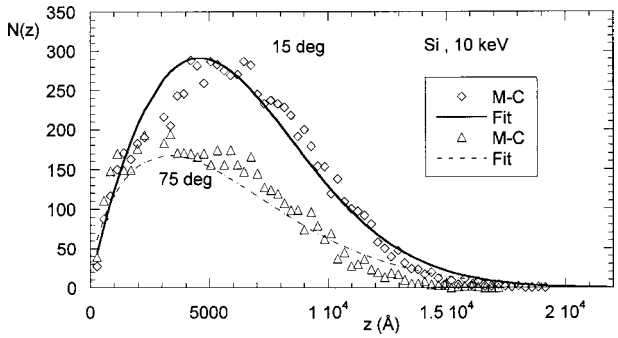

Fig. 6b. Typical implantation profiles of positrons at 10 keV (incident angles 15° and 75°) in the semi-infinite Si.

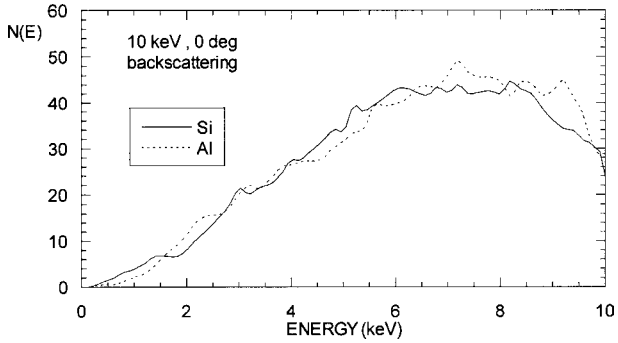

Fig. 7. Comparison of energy distributions of backscattered positrons from the semi-infinite Al and Si targets at 10 keV positron energy andat incident angles of 0°.

similar to each other with a slight variation, and the backscattering coefficients from silicon and aluminum are nearly equal.

The Monte Carlo simulation of the scattering processes of penetrating positrons in solids was described. In this calculation, the scattering processes consist of elastic and inelastic scattering. The calculation provided the energy and angular distributions of transmitted and backscattered positrons for silicon by the Monte Carlo approach. The results were found to be useful for the theoretical description of positron penetration and worthy of further development.

References

1. Aydın A (2000) Total cross sections for elastic scattering of positrons for silicon, gallium and antimony atoms. J Instrum Sci Tech Balıkesir University 2:47–57
2. Aydın A (2002) Monte Carlo simulation of kilovolt positron penetration and backscattering probabilities in solids. Nucl Instrum Meth B 197:11–16
3. Baker JA, Chilton NB, Jensen KO, Walker AB, Coleman PG (1991) Material dependence of positron implantation depth. J Phys-Condens Matter 3:4109–4114
4. Berger MJ (1991) Differences in the multiple scattering of positrons and electrons. Appl Radiat Isot 42;10:905–916
5. Bouarissa N, Walker AB, Aourag H (1998) Backscattering of slow positron from semi-infinite aluminum. J Appl Phys 83;7:3643–3648
6. Fernández-Varea JM, Liljequist D, Csillag S, Räty R, Salvat F (1996) Monte Carlo simulation of 0.1–100 keV electron and positron transport in solids using optical data and partial wave methods. Nucl Instrum Meth B 108:35–50
7. Gryzinski M (1965) Classical theory of atomic collisions. Phys Rev A 138:305–358
8. Kotera M, Murata K, Nagami K (1981) Monte Carlo simulation of 1–10 keV electron scattering in an aluminum target. J Appl Phys 52;12:7403–7408
9. Liljequist D (1983) A simple calculation of inelastic mean free path and stopping power for 50 eV – 50 keV electrons in solids. J Phys D: Appl Phys 16:1567–1582
10. Mäkinen J, Palko S, Martikainen J, Hautojärvi P (1992) Positron backscattering probabilities from solid surfaces at 2–30 keV. J Phys-Condens Matter 4:L503–L508
11. Massoumi GR, Lennard WN, Schultz PJ, Porcelli TA, Simpson PJ (1995) Energy loss measurements for 20 keV positrons in Al thin films. Appl Surf Sci 85:39–42
12. Mills AP, Wilson RJ (1982) Transmission of 1–6 keV positrons through thin metal films. Phys Rev A 26;1:490–500
13. Mott NF, Massey HSW (1987) The theory of atomic collisions, 3rd ed. Oxford University Press, New York
14. Nigam BP, Mathur VS (1961) Difference in the multiple scattering of electrons and positrons. Phys Rev 121:1577–1580
15. Özmutlu EN, Aydın A (1994) Monte Carlo calculations of 50 eV – 1 MeV positrons in aluminum. Appl Radiat Isot 45;9:963–971
16. Press WH, Flannery BP, Teukolsky SA, Vetterling WT (1986) Numerical recipes. Cambridge University Press, New York
17. Seltzer SM (1991) Electron-photon Monte-Carlo calculations: the ETRAN code. Appl Radiat Isot 42:917–941
18. Shimuzu R, Ichimura S (1983) Direct Monte Carlo simulation of scattering processes of kV electrons in aluminum; comparison of theoretical N(E) spectra with experiment. Surf Sci 133:250–266